 CMES, vol.14, no.2, pp.129-140, 2006

Sequential Limit Analysis of Rotating Hollow Cylinders of Nonlinear Isotropic Hardening

S.-Y. Leu[1] and J.T. Chen[2]

Abstract: Plastic limit angular velocity of rotating hollow cylinders made of the von Mises materials with nonlinear isotropic hardening is investigated numerically and analytically in the paper. The paper applies sequential limit analysis to deal with the rotating problems involving hardening material property and weakening behavior resulted from the widening deformation. By sequential limit analysis, the paper treats the plasticity problems as a sequence of limit analysis problems stated in the upper bound formulation. Rigorous upper bounds are acquired iteratively through a computational optimization procedure with the angular velocity factor as the objective function. Especially, rigorous validation was conducted by numerical and analytical studies of rotating hollow cylinders in terms of the plastic limit angular velocity as well as the onset of instability. It is found that the computed limit angular velocities are rigorous upper bounds and agree very well with the analytical solutions.

keyword: Sequential limit analysis, Plastic limit angular velocity, Rotating cylinder, von Mises criterion, Nonlinear strain-hardening, Instability.

1 Introduction

Plastic limit angular velocity of cylinders is useful information requested frequently for an optimal structural design. Much effort, see Davis and Connelly (1959), Lenard and Haddow (1972), Nadai (1950), Rimrott (1960), has been made to such important topics by investigting the elastic-plastic behavior and the fully plastic state. Similar attention, see Alexandrova and Alexandrov (2004), Eraslan and Argeso (2002), Güven (1997), Ma, Hao and Miyamoto (2001), Orcan and Eraslan (2002), is also paid to the limit angular velocity of disks. However, efficient and accurate computational optimization procedures for investigating such problems of optimization feature are still in need for general and effective considerations of cylinders or disks optimal design.

As it is well known that limit analysis is effective to set a rigorous bound on the asymptotic behavior of an elastic-plastic material by the lower bound or the upper bound theorem. Moreover, limit analysis seems to play the role of a snapshot look at the structural performance of rotating cylinders by efficiently providing the limit solution based on only simple input data. On the other hand, it is sequential limit analysis with a sequence of limit analysis problems conducted sequentially suitable for the large deformation analysis, see Corradi, Panzeri and Poggi (2001), Corradi and Panzeri (2004), Huh and Lee (1993), Huh, Lee and Yang (1999), Hwan (1997), Leu (2003), Leu (2005), Yang (1993), with updating local yield criteria in addition to the configuration of the deforming structures while conducting a sequence of limit analysis problems sequentially. In each step and therefore the whole deforming process, rigorous upper bound or lower bound solutions are supposedly acquired sequentially as to bound the real limit solutions.

Actually, not only can we establish theoretically the equality relation between the greatest lower bound and the least upper bound by duality theorems, see Yang (1991a), Yang (1993), but also we can acquire numerically the limit results efficiently and accurately by the use of finite element methods, see Reddy (1993), together with mathematical programming techniques, see Luenberger (1984) , Zhu, Liu, Wang and Yu (2004). Furthermore, it is possible to assure the accuracy of limit analysis or sequential limit analysis and extend its applicability to more complex problems in engineering applications with the aid of finite-element methods together with an appropriate numerical algorithm. Especially, a combined smoothing and successive approximation (CSSA) algorithm presented by Yang (1982) has been utilized successfully, with satisfactory results at a modest cost, in certain problems of limit analysis, see

[1] Hydraulic Engineering Department, Sinotech Engineering Consultants, Ltd., 171 Sec. 5 Nanking E. Rd., Taipei 105, Taiwan. Email: syleu@mail.sinotech.com.tw

[2] Distinguished Professor, Department of Harbor and River Engineering, National Taiwan Ocean University, Keeling, Taiwan.

Huh and Yang (1991) and sequential limit analysis, see Huh and Lee (1993), Huh, Lee and Yang (1999), Hwan (1997), Leu (2003), Leu (2005), Yang (1993). Its unconditional convergence and numerical accuracy have been demonstrated by practical applications. It is noted that sophisticated constitutive models are considered to model more realistic materials, see Haghi and Anand (1991), Karšaj, Sansour and Sorić (2004), Le Tallec (1986), Liu (2005). Accordingly, its convergence analysis was recently performed and validation was also conducted rigorously while extending the CSSA algorithm further to sequential limit analysis of viscoplastic problems, see Leu (2003), or involving materials with nonlinear isotropic hardening, see Leu (2005).

The paper aims to apply sequential limit analysis to investigate the plastic limit angular velocity of rotating hollow cylinders of the von Mises materials with nonlinear isotropic strain-hardening. By sequential limit analysis, the paper is to treat the plasticity problems as a sequence of limit analysis problems stated in the upper bound formulation seeking the least upper bound of the plastic angular velocity involving the prescribed action of internal and/or external pressure. Especially, it implies the numerical challenges facing the treatment of material hardening and weakening behavior induced by the widening deformation.

2 Problem formulation

2.1 Lower bound formulation

The hollow cylinder is considered to rotate about its axis at constant angular velocityω. It is assumed that the angular velocity varies very slowly such that the angular acceleration is negligible. We consider the plane-strain problem with the domain D consisting of the static boundary ∂D_s and the kinematic boundary ∂D_k. The problem is to seek the maximum allowable angular velocity factor $\rho\omega^2(\sigma)$ under constraints of static and constitutive admissibility such that

$$\begin{aligned}
&\text{maximize} && \rho\omega^2(\sigma)\\
&\text{subject to} && \nabla\cdot\sigma+\rho\omega^2\vec{r}=0 \quad \text{in } D\\
&&& \sigma\cdot\vec{n}=q_{s1}\vec{t}_{s1} \quad \text{on } \partial D_{s1}\\
&&& \sigma\cdot\vec{n}=q_{s2}\vec{t}_{s2} \quad \text{on } \partial D_{s2}\\
&&& \|\sigma\|_{\vee}\le\sigma_Y(\bar{\varepsilon}) \quad \text{in } D\\
&&& \partial D_s=\partial D_{s1}\cup\partial D_{s2}
\end{aligned} \tag{1}$$

where ρ is the constant material density of the rotating hollow cylinders, ω is the angular velocity, $\rho\omega^2\vec{r}$ is the centrifugal force with $\vec{r}$ the position vector, $\vec{n}$ indicates the unit outward normal vector of the boundary and the traction vectors $\vec{q}_{s1}$, $\vec{q}_{s2}$ are the prescribed loads on the boundaries ∂D_{s1} , ∂D_{s2}, respectively; $\|\sigma\|_{\vee}$denotes the von Mises primal norm on stress tensor σ and the current yield stress σ_Y is a function of the equivalent strain $\bar{\varepsilon}$ describing isotropic hardening. Therefore, this constrained problem is to sequentially maximize the angular velocity factor $\rho\omega^2(\sigma)$, representing the magnitude of the driving load, in each step corresponding to $\sigma_Y(\bar{\varepsilon})$. Obviously, the problem statement leads naturally to the lower bound formulation seeking the greatest lower bound on statically admissible solutions.

2.2 Upper bound formulation

Now we are to transform the lower bound formulation to the upper bound formulation as similar to the previous work of Huh and Yang (1991). Equilibrium equations can be restated in a weak form as

$$\int_D \vec{u}\cdot\left(\nabla\cdot\sigma+\rho\omega^2\vec{r}\right)dA=0 \tag{2}$$

where $\vec{u}$ is a kinematically admissible velocity field. Integrating by parts, using the divergence theorem and imposing static boundary conditions, we may rewrite Eq. (2) to give an expression for $\rho\omega^2(\sigma)$ as

$$\begin{aligned}
\int_D \vec{u}\cdot(\rho\omega^2\vec{r})dA &= \rho\omega^2(\sigma)\int_D \vec{u}\cdot\vec{r}\,dA\\
&= \int_D \sigma:\dot{\varepsilon}dA-\int_{\partial D_{s1}}\vec{u}\cdot\vec{q}_{s1}dS-\int_{\partial D_{s2}}\vec{u}\cdot\vec{q}_{s2}dS
\end{aligned} \tag{3}$$

where $\dot{\varepsilon}$ is the strain rate tensor. Since $\vec{u}$ appears homogeneously and linearly in Eq. (3), we can normalize the equation by setting the following normalization

$$\int_D \vec{u}\cdot\vec{r}\,dA=1 \tag{4}$$

which is to be treated as one of constraints. Note that, the normalization condition involving the velocity field is imposed on the whole domain. In the previous works, e.g. Huh and Yang (1991), Leu (2003, 2005), the normalization condition was, in stead, simply related to the velocity filed prescribed along some boundaries.

Notice that the power $\sigma:\dot{\varepsilon}$ is nonnegative, it implies $\sigma:\dot{\varepsilon}=|\sigma:\dot{\varepsilon}|$. Further, according to a generalized Hölder

inequality, see Yang (1991b), and the normality condition in plasticity, see Drucker (1959), it results in

$$\sigma : \dot{\varepsilon} = |\sigma : \dot{\varepsilon}| \leq \|\sigma\|_{\vee} \|\dot{\varepsilon}\|_{-\vee} \tag{5}$$

where $\|\dot{\varepsilon}\|_{-\vee}$ is the dual norm, see Huh and Yang (1991), of $\|\sigma\|_{\vee}$ based on the flow rule associated with the von Mises yield criterion. Therefore, $\rho\omega^2(\sigma)$ can be bounded above by $\rho\overline{\omega}^2\left(\vec{u}\right)$ as

$$\begin{aligned}\rho\omega^2(\sigma) &= \int_D \sigma : \dot{\varepsilon} - \int_{\partial D_{s1}} \vec{u}\cdot\vec{q}_{s1}\,dS - \int_{\partial D_{s2}} \vec{u}\cdot\vec{q}_{s2}\,dS \\ &\leq \int_D \|\sigma\|_{\vee}\|\dot{\varepsilon}\|_{-\vee}\,dA - \int_{\partial D_{s1}} \vec{u}\cdot\vec{q}_{s1}\,dS - \int_{\partial D_{s2}} \vec{u}\cdot\vec{q}_{s2}\,dS \\ &= \rho\overline{\omega}^2\left(\vec{u}\right)\end{aligned} \tag{6}$$

Thus, the upper bound formulation is stated in the form of a constrained minimization problem as

$$\begin{aligned}&\text{minimize} \quad \rho\overline{\omega}^2\left(\vec{u}\right) \\ &\text{subject to} \quad \rho\overline{\omega}^2\left(\vec{u}\right) = \textstyle\int_D \|\sigma\|_{\vee}\|\dot{\varepsilon}\|_{-\vee}\,dA \\ &\qquad\qquad - \int_{\partial D_{s1}} \vec{u}\cdot\vec{q}_{s1}\,dS - \int_{\partial D_{s2}} \vec{u}\cdot\vec{q}_{s2}\,dS \\ &\qquad\qquad \textstyle\int_D \vec{u}\cdot\vec{r}\,dA = 1 \quad \text{in } D \\ &\qquad\qquad \nabla\cdot\vec{u} = 0 \quad \text{in } D \\ &\text{kinematic boundary conditions on } \partial D_k\end{aligned} \tag{7}$$

where $\nabla\cdot\vec{u} = 0$ is the incompressibility constraint inherent in the von Mises model. Therefore, the upper bound formulation seeks the least upper bound on kinematically admissible solutions.

Note that the primal-dual formulations (1) and (7) are convex programming problems, see Huh and Yang (1991), Yang (1993). Thus, for each step, there exist unique maximizer and minimizer to Problems (1) and (7), respectively. Therefore, the extreme values of the lower bound functional $\rho\omega^2(\sigma)$ and its corresponding upper bound functional $\rho\overline{\omega}^2\left(\vec{u}\right)$ are equal to the unique, exact solution $\rho\omega^{*2}$ for each step in a process. Namely

$$\text{maximize } \rho\omega^2(\sigma) = \rho\omega^{*2} = \text{ minimize } \rho\overline{\omega}^2\left(\vec{u}\right) \tag{8}$$

2.3 Discretized and augmented functional

To discretize the continuous domain and surface boundary, we adopt four-node quadrilateral isoparametric elements, see Reddy (1993). Applying finite-element discretization, the original functional in the problem equation (7) is approximated by a new one in a finite-dimensional space of the vector $\{U\}$, the discrete approximation of the velocity field. We restate the problem as

$$\begin{aligned}&\text{minimize} \quad \rho\tilde{\omega}^2(\{U\}) = \sum_{e=1}^{N_e} \sigma_Y(\overline{\varepsilon})\sqrt{\{U\}^t[K_{e1}]\{U\}} \\ &\qquad\qquad - \sum_{se1=1}^{N_{s1}} \{U\}^t\{Q_{se1}\} - \sum_{se2=1}^{N_{s2}} \{U\}^t\{Q_{se2}\} \\ &\text{subject to} \quad \{U\}^t\{R\} = 1 \\ &\qquad\qquad \{U\}^t\{C\} = 0\end{aligned} \tag{9}$$

where N_e , N_s denote the numbers of elements used to discretize the domain and surface boundary respectively; the superscript t denotes transposition; $\{Q_{se1}\}$ and $\{Q_{se2}\}$ are the nodal-point force vectors corresponding to $\vec{q}_{s1}$ and $\vec{q}_{s2}$, respectively; $[K_{e1}]$ is the element stiffness matrix, $\{C\}$ and $\{R\}$ are vectors.

To deal with the constrained minimization problem equation (9), we utilize the penalty function method, see Reddy (1986), and the Lagrangian multiplier method, see Reddy (1986), to relax the incompressibility constraint and to impose the normalization condition. The corresponding unconstrained minimization problem is then expressed as

$$\text{minimize} \quad \rho\tilde{\omega}^2(\{U\}) + \frac{\beta}{2}p(\{U\}) - \lambda(\{U\}^t\{R\} - 1) \tag{10}$$

$$\text{with } p(\{U\}) = \sum_{e=1}^{N_e} \{U\}^t[K_{e2}]\{U\}$$

where the penalty parameter β is a sufficiently large positive constant, λ is the Lagrangian multiplier, and $[K_{e2}]$ is the coefficient matrix corresponding to the incompressibility constraint. It is noted that the element stiffness matrix $[K_{e1}]$ is positive semi-definite such that the objective functional is non-smooth over some rigid regions. The resulting numerical difficulty is to be overcome in the next section.

3 Computations

To solve the minimization problem equation (10), we apply the necessary condition for the minimum of

$\rho\tilde{\omega}^2(\{U\}) + \frac{\beta}{2}p(\{U\}) - \lambda(\{U\}^t\{R\} - 1)$, namely taking its first derivative with respect to $\{U\}$, and the Lagrangian multiplier λ, respectively. Moreover, the objective functional is smoothed by a small real number δ to overcome the numerical difficulty resulting from non-smoothness over some rigid regions as detailed by Huh and Yang (1991). Reorganizing the nonlinear equations, linear matrix-vector equations are then produced as

$$[K]\{U\} = \lambda\{R\} + \{Q_{s1}\} + \{Q_{s2}\} \tag{11}$$

$$\{U\}^t\{R\} - 1 = 0 \tag{12}$$

with

$$[K]\{U\} = \sum_{e=1}^{N_e} \sigma_Y(\overline{\varepsilon}^n) \frac{[K_{e1}]\{U\}_{j+1}}{\sqrt{\{U^*\}_j^t [K_{e1}]\{U^*\}_j + \delta^2}} + \beta \sum_{e=1}^{N_e} [K_{e2}]\{U\}_{j+1}$$

$$\{Q_{s1}\} = \sum_{se1=1}^{N_{s1}} \{Q_{se1}\}$$

$$\{Q_{s2}\} = \sum_{se2=1}^{N_{s2}} \{Q_{se2}\}$$

where subscriptions j, $(j+1)$ indicate quantities corresponding to any successive iterations. At the first step, we have the equivalent strain rate $\overline{\varepsilon}^1 = 0$. For the current step $n \geq 2$, the value of $\overline{\varepsilon}^n$ is obtained as the following expression

$$\overline{\varepsilon}^n = \sum_{i=1}^{n-1} \dot{\varepsilon}_i \Delta t_i \tag{13}$$

where Δt_i is the step size.

Combining Eqs. (11) and (12), we express λ, $\{U\}$ in each step as follows

$$\lambda = \frac{1 - \{R\}^t [K]^{-1} (\{Q_{s1}\} + \{Q_{s2}\})}{\{R\}^t [K]^{-1} \{R\}} \tag{14}$$

$$\{U\} = \lambda [K]^{-1}\{R\} + [K]^{-1}(\{Q_{s1}\} + \{Q_{s2}\}) \tag{15}$$

where $[K]^{-1}$ is the inverse of $[K]$.

As expressed in Eq. (14), the current value of λ_{j+1} is based on the value of $\{U^*\}_j$ obtained at the preceding iteration j. With the acquired λ_{j+1}, the other unknown $\{U\}_{j+1}$ is then calculated as expressed in Eq. (15). In the beginning, an arbitrary $\{U\}_0$ is assumed as the initial estimate. A convergent sequence of $\lambda(\{U^*\}_j)$ is then generated iteratively and converges to the plastic limit angular velocity. Computationally, an inner and outer iterative sequence is conducted to solve the minimization problem. From one outer iteration to the next, the smoothing parameter δ used in the inner iteration is allowed to decrease and then convergence to zero finally. Stopping criterion based on the ratio of Euclidean norms $E_u = \left\|\{U^*\}_j - \{U^*\}_{j-1}\right\|_2 / \left\|\{U^*\}_{j-1}\right\|_2$ is applied to check the convergence of each step.

All the abovementioned procedures are summarized as the flowchart shown in Figure 1.

4 Numerical examples

The paper is aimed to apply sequential limit analysis to the plastic limit angular velocity of hollow cylinders involving strain-hardening materials in plane-strain conditions. In the formulation, the action of angular velocity contributes to the driving load to cause the rotating cylinders fully plastic. Comparisons between numerical results and analytical solutions are made as to show the reliable applications. In the computations, the present paper adopts the Voce hardening law

$$\sigma_Y = \sigma_\infty - (\sigma_\infty - \sigma_0)\exp(-h\overline{\varepsilon}) \tag{16}$$

where σ_0 is the initial yield strength, σ_∞ is the saturation stress, h is the hardening exponent. For the sake of rigorous validation, analytical solutions for the angular velocity are derived as detailed in Appendix A. To be complete, the onset of the instability is also study analytically in Appendix B.

In the numerical examples, the initial inner and outer radii are denoted as a_0 and b_0, respectively. The angular velocity required to keep the deforming cylinder fully plastic is then computed sequentially by using the CSSA algorithm. In the following case studies, we adopt the following non-dimensional parameters: $a_0 = 5.0$, $b_0 = 10.0$, $h = \sqrt{3}$ and a constant step size $\Delta t = 1.0$.

As shown in Figure 1, only one quarter of the axisymmetric structure is simulated. Four-node bilinear quadrilateral isoparametric elements are utilized to discretize the problem domain without numerical difficulties. As mentioned by Huh, Lee and Yang (1999), however, the successful choice of the linear element may depend on the

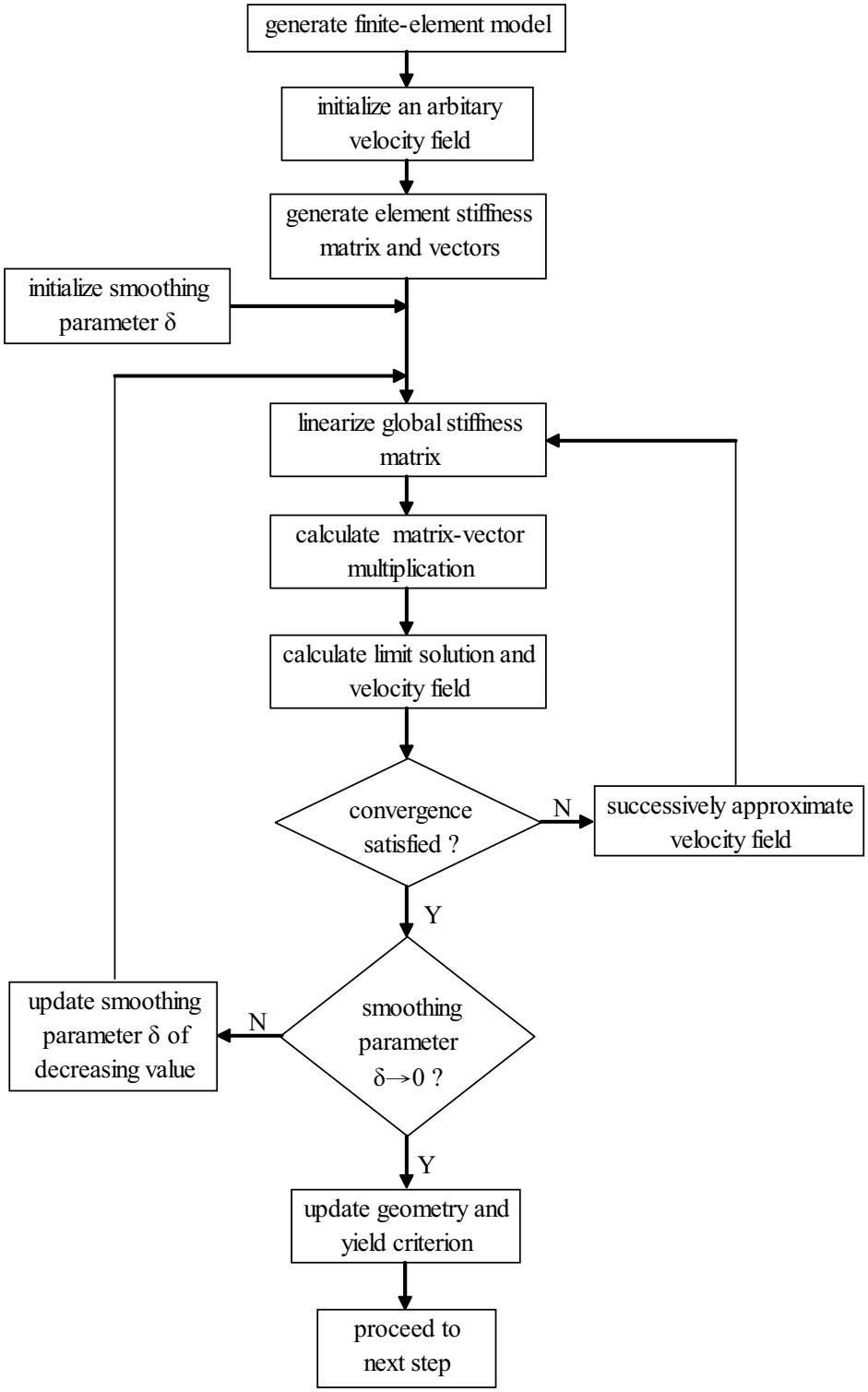

Figure 1 : Flowchart of the computational procedures

nature of a problem. The finite element mesh of 15×25 elements shown in Figure 2 is adopted in the following computations. In the beginning, the first-step limit angular velocity is obtained. The first-step solution is the

limit value of the angular velocity causing the cylinder of dimensions a_0 and b_0 fully plastic. Following the first step, each step in sequential limit analysis starts with the result obtained in the preceding step. A sequence of limit analysis problems is then solved to obtain sequential numerical solutions of the rotating problem.

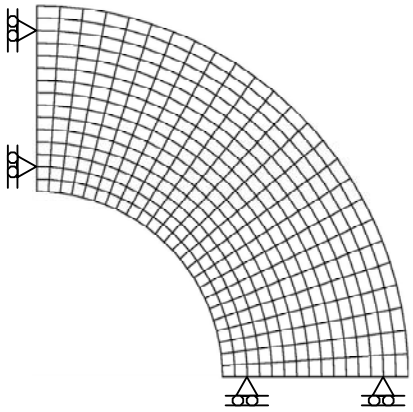

Figure 2 : Schematic finite-element model for a rotating hollow cylinder

Firstly, we consider the rotating cylinder free of any action of internal or external pressure. Accordingly, the computed first-step limit angular velocity factor $\rho\omega^2$, normalized by σ_0/b_0^2, is 2.13622 with the convergence tolerance $E_u = 0.00001$ compared to 2.13434 by Eq. (38) in Appendix. A sequence of limit analysis problems is then solved to obtain sequential numerical solutions of the rotating problem. Parametric studies are performed with various values of $R = \sigma_\infty/\sigma_0$. The results normalized by σ_0/b_0^2 are summarized in Figure 3. All the computed upper bounds agree very well with the analytical solutions at a modest cost.

Secondly, the combination action of internal and external pressure is also considered. In the following computations, the values of internal and external pressure are prescribed constants. Accordingly, we still consider a problem of widening deformation with the angular velocity contributing to the driving load. As shown in Eqs. (37) and (38) in Appendix A, the action of internal pressure is to reduce the plastic limit angular velocity while the action of external pressure is to increase the plastic limit angular velocity. Figure 4 shows the effect of $(P_i - P_o)/\sigma_0$ with various values on the plastic limit angular velocity. Again, the computed upper bounds are in good agreement with the analytical solutions.

On the other hand, as shown in Figures 3∼4 and the analytical solutions derived in Appendix B, the rotating hollow cylinders of $\sigma_\infty/\sigma_0 > 2$ are strengthened due to the strain-hardening described by the Voce hardening law with $h = \sqrt{3}$ until the onset of instability. Following that, however, the weakening phenomenon is observed while the effect of widening deformation counteracts that of the strain-hardening. Note that, the onset of instability concerned is about the plastic instability marked by the rotating speed maximum while dealing with thick-walled cylinders, see Rimrott (1960), Chakrabarty (1987). Namely, the strengthening due to material hardening is exceeded by the weakening resulted from the widening deformation, see Rimrott (1960). The effect of the hardening index on the strengthening/weakening phenomenon is as shown in Figure 5 with $\sigma_\infty/\sigma_0 = 2$. The higher the hardening index value is, the more significant hardening phenomenon can be observed.

As detailed in Appendix B, the onset of instability can be calculated by the following mathematical condition

$$\frac{\partial(\rho\omega^2 b_0^2/\sigma_0)}{\partial a} = 0 \tag{17}$$

Thus, the onset of instability, corresponding to the initial inner and outer radii a_0, b_0 and the strain-hardening described by the Voce hardening law with $h = \sqrt{3}$, can be shown as follows:

$$\frac{a}{a_0} = \sqrt{\frac{(b_0/a_0)^2 - 1}{X - 1}} \tag{18}$$

with the change of variables as follows

$$X = \frac{\overline{A} + \sqrt{\overline{A}^2 + 4(b_0/a_0)^2}}{2} \tag{19}$$

$$\overline{A} = \frac{(b_0/a_0)^2 - 1}{(\sigma_\infty/\sigma_0 - 1)} \tag{20}$$

Note that, considering the strain-hardening described by the Voce hardening law with $h = \sqrt{3}$, the stability condition for the widening problem of rotating hollow cylinders is $\sigma_\infty/\sigma_0 > 2$ regardless of the geometry of rotating hollow cylinders as detailed in Appendix B. Figure 6 shows the relationship between the onset of instability and $R = \sigma_\infty/\sigma_0$ with various values of b_0/a_0 for $\sigma_\infty/\sigma_0 \geq 2$. Again, the computed results for the onset of instability agree very well with the analytical solutions as shown in Figure 4 and Figure 6.

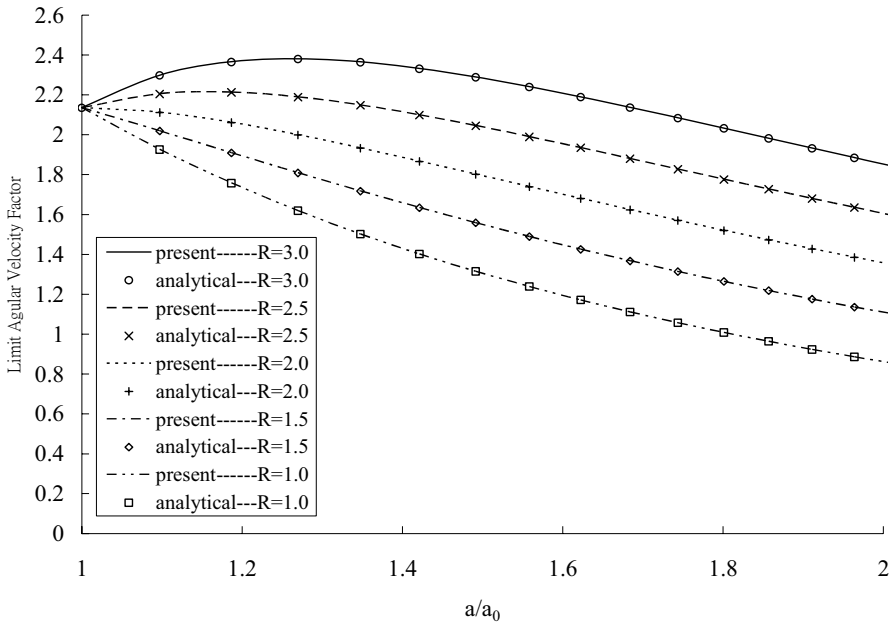

Figure 3 : Plastic limit angular velocity factor $\rho\omega^2 b_0^2/\sigma_0$ vs. inner radius a/a_0 with $R = \sigma_\infty/\sigma_0$

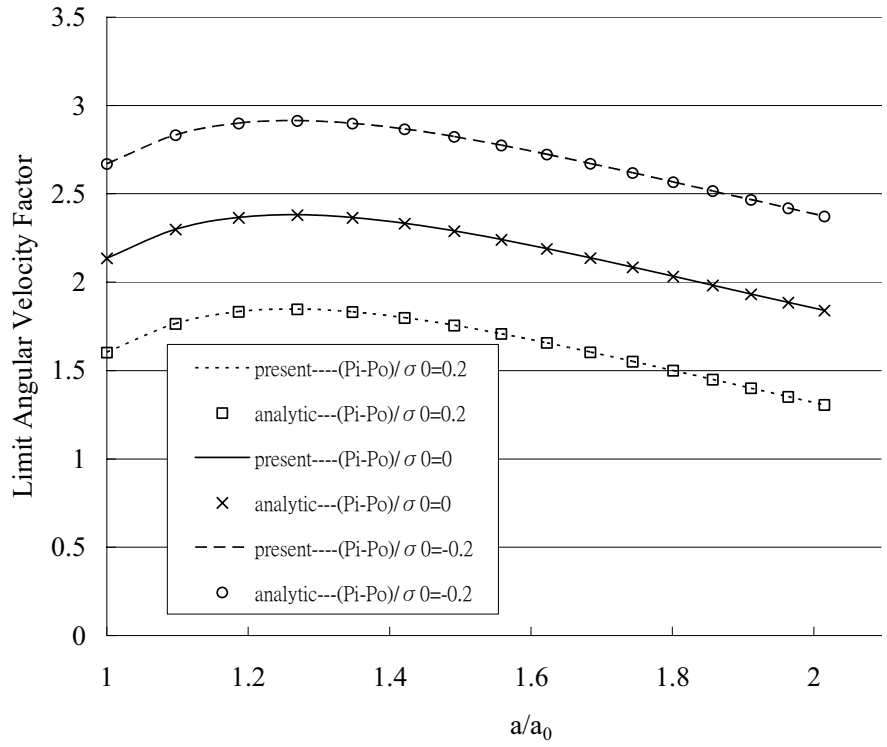

Figure 4 : Effect of internal and outer pressure on plastic limit angular velocity factor $\rho\omega^2 b_0^2/\sigma_0$ with $\sigma_\infty/\sigma_0 = 3$

5 Conclusions

The problem seeking plastic limit angular velocity of rotating hollow cylinders is of optimization feature and is encountered frequently for optimal structural design. By utilizing sequential limit analysis, the paper deals with rotating hollow cylinders made of the von Mises mate-

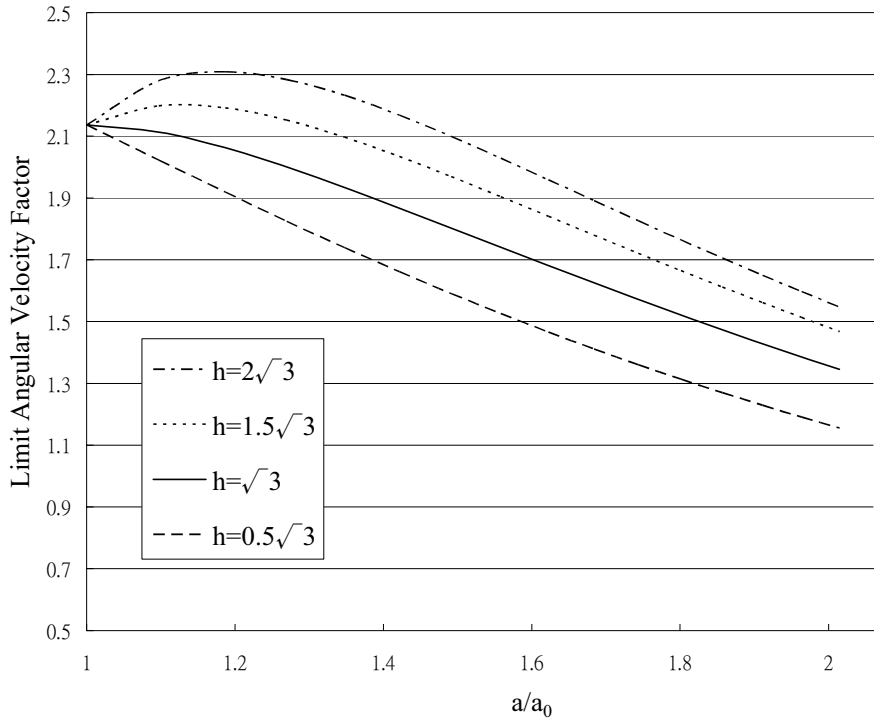

Figure 5 : Effect of the hardening index on strengthening/weakening behavior with $\sigma_\infty/\sigma_0 = 2$

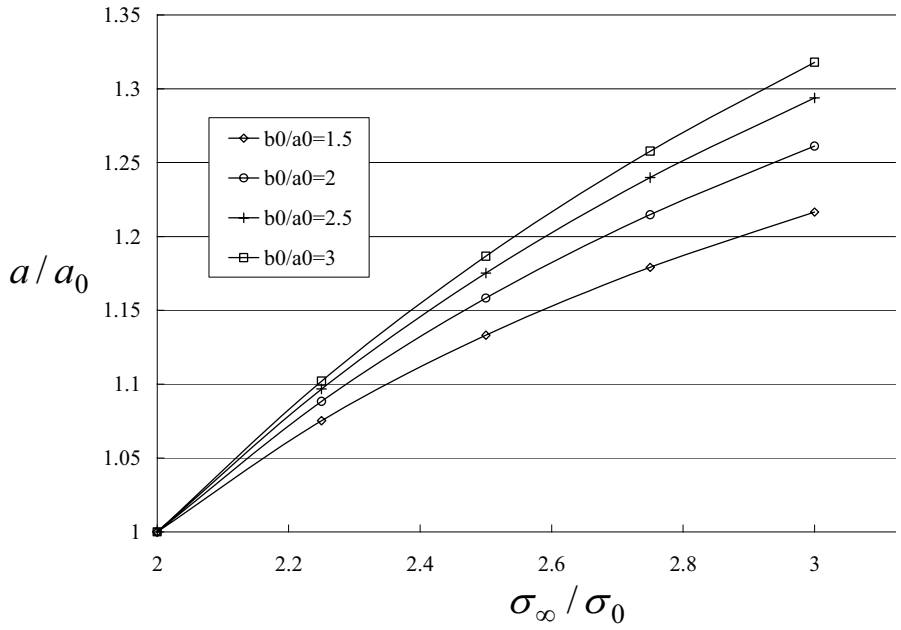

Figure 6 : The onset of instability a/a_0 **vs.** σ_∞/σ_0

rials with nonlinear isotropic hardening. The plasticity problem was then formulated as a sequence of limit analysis problems stated in the upper bound formulation with the angular velocity factor as the objective function. In addition, the action of prescribed internal and/or external pressure was also considered. Specifically, the cor-

responding normalization condition is imposed on the whole domain. Finally, the limit angular velocity, contributing to the driving load, was expressed in a simplified formulation.

Numerically, rigorous upper bounds are acquired iteratively through a computational optimization procedure based on a general algorithm involving inner and outer iterations. The general algorithm is comparable for its simple implementation, unconditional convergence. Analytic solutions of the plastic limit angular velocity and the onset of instability corresponding to the Voce hardening law was also derived in the paper for rigorous comparisons.

Numerical and analytically studies of rotating hollow cylinders have demonstrated the accuracy of the numerical procedure presented here. Especially, the computed upper-bound results are in good agreement with analytical solutions at a modest cost.

References

Alexandrova, N.; Alexandrov, S. (2004): Elastic-plastic distribution in a rotating annular disk. *Mechanics Based Design of Structures and Machines*, vol. 32, pp. 1-15.

Chakrabarty, J. (1987): *Theory of Plasticity*, McGraw-Hill, New York.

Corradi, L.; Panzeri, N.; Poggi, C. (2001): Post-critical behavior of moderately thick axisymmetric shells: a sequential limit analysis approach. *International Journal of Structural Stability and Dynamics*, vol. 1, pp. 293-311.

Corradi, L.; Panzeri, N. (2004): A triangular finite element for sequential limit analysis of shells. *Advances in Engineering Software*, vol. 35, pp. 633-643.

Davis, E. A.; Connelly, F. M. (1959): Stress distribution and plastic deformation in rotating cylinders of strain-hardening material. *Journal of Applied Mechanics*, vol. 26, pp. 25-30.

Drucker, D. C. (1959): A definition of stable inelastic material in the mechanics of continua. *Journal of Applied Mechanics*, vol. 81, pp. 101-106.

Eraslan, A. N.; Argeso, H. (2002): Limit angular velocity of variable thickness rotating disks. *International Journal of Solids and Structures*, vol. 39, pp. 3109-3130.

Güven, U. (1997): The fully plastic rotating disk with rigid inclusion. *ZAMM*, vol. 77, pp. 714-716.

Haghi, M.; Anand, L. (1991): Analysis of strain-hardening viscoplastic thick-walled sphere and cylinder under external pressure. *International Journal of Plasticity*; vol. 7, pp. 123-140.

Huh, H.; Yang, W. H. (1991): A general algorithm for limit solutions of plane stress problems. *International Journal of Solids and Structures*, vol. 28, pp. 727-738.

Huh, H.; Lee, C. H. (1993): Eulerian finite-element modeling of the extrusion process for working-hardening materials with the extended concept of limit analysis. *Journal of Materials Processing Technology*, vol. 38, pp. 51-62.

Huh, H.; Lee, C. H.; Yang, W. H. (1999): A general algorithm for plastic flow simulation by finite element limit analysis. *International Journal of Solids and Structures*, vol. 36, pp. 1193-1207.

Hwan, C. L. (1997): An upper bound finite element procedure for solving large plane strain deformation. *International Journal for Numerical Methods in Engineering*, vol. 40, pp. 1909-1922.

Karšaj, I.; Sansour, C.; Sorić, J. (2004): A new free energy-based model of the kinematic hardening in large strain elastoplasticity. *CMES: Computer Modeling in Engineering & Sciences*, Vol. 8, pp. 45-60.

Lenard, J.; Haddow, J. B. (1972): Plastic collapse speeds for rotating cylinders. *International Journal of Mechanical Sciences*, vol. 14, pp. 285-292.

Le Tallec, P. (1986): Numerical solution of viscoplastic flow problems by augmented Lagrangians. *IMA Journal of Numerical Analysis*, vol. 6, pp. 185-219.

Leu, S.-Y. (2003): Limit analysis of viscoplastic flows using an extended general algorithm sequentially: convergence analysis and validation. *Computational Mechanics*, vol. 30, pp. 421-427.

Leu, S.-Y. (2005): Convergence analysis and validation of sequential limit analysis of plane-strain problems of the von Mises model with nonlinear isotropic hardening. *International Journal for Numerical Methods in Engineering*, vol. 64, pp. 322-334.

Liu, C.-S. (2005): Computational applications of the Poincaré group on the elastoplasticity with kinematic hardening. *CMES: Computer Modeling in Engineering & Sciences*, Vol. 8, pp. 231-258.

Luenberger, D. G. (1984): *Linear and Nonlinear Programming*, Addison-Wesley, MA.

Ma, G.; Hao, H.; Miyamoto, Y. (2001): Limit angular velocity of rotating disk with unified yield criterion. *International Journal of Mechanical Science*, vol. 43, pp. 1137-1153.

Nadai, A. (1950): *Theory of Flow and Fracture of Solids*, McGraw-Hill, New York.

Orcan, Y.; Eraslan, A. N. (2002): Elastic-plastic stresses in linearly hardening rotating solid disks of variable thickness. *Mechanics Research Communications*, vol. 29, pp. 269-281.

Reddy, J. N. (1986): *Applied Functional Analysis and Variational Methods in Engineering*. McGraw-Hill, New York.

Reddy, J. N. (1993): *An Introduction to the Finite Element Method*, McGraw-Hill, New York.

Rees, D. W. A. (1999): Elastic-Plastic Stresses in Rotating Discs by von Mises and Tresca. *ZAMM*, vol. 79, pp. 281-288.

Rimrott, F. P. J. (1960): On the plastic behavior of rotating cylinders. *Journal of Applied Mechanics*, vol. 27, pp. 309-315.

Yang, W. H. (1982): A variational principle and an algorithm for limit analysis of beams and plates. *Computer Methods in Applied Mechanics and Engineering*, vol. 33, pp. 575-582.

Yang, W. H. (1991a): Admissibility of discontinuous solutions in mathematical models of plasticity. In: W. H. Yang (ed) *Topics in Plasticity*, AM Press, MI, pp. 241-260.

Yang, W. H. (1991b): On generalized Hölder inequality. *Non-linear Analysis, Theory, Methods & Applications*,vol. 16, pp. 489-498.

Yang, W. H. (1993): Large deformation of structures by sequential limit analysis. *International Journal of Solids and Structures*, vol. 30, pp. 1001-1013.

Zhang, Y.-G.; Zhang P.; Xue W.-M. (1994): Limit analysis considering initial constant loadings and proportional loadings. *Computational Mechanics*, vol. 14, pp. 229-234.

Zhu, Z. Q.; Liu, Z. ; Wang, X. L.; Yu, R. X. (2004) Construction of integral objective function/fitness function of multi-objective/multi-disciplinary optimization. *CMES: Computer Modeling in Engineering & Sciences*, Vol. 6, pp. 567-576.

Appendix A:

We consider a plane-strain problem with a rotating hollow cylinder simulated by the von Mises model with nonlinear isotropic hardening. The cylinder has its initial interior and exterior radii denoted by a_0 and b_0. As shown in the Eq. (1), the rotating hollow cylinder may be subjected to internal and/or external pressure in addition to the centrifugal force $\rho\omega^2\vec{r}$. In the following derivation, the values of internal and external pressure are considered constant. Accordingly, we consider a problem of widening deformation with the centrifugal force being the driving load.

The behavior of nonlinear isotropic hardening is described by the Voce hardening law

$$\begin{aligned}\sigma_Y &= \sigma_0 + (\sigma_\infty - \sigma_0)\,[1 - \exp(-h\bar{\varepsilon})] \\ &= \sigma_\infty - (\sigma_\infty - \sigma_0)\exp(-h\bar{\varepsilon})\end{aligned} \tag{21}$$

where σ_∞ is the saturation stress and h is the hardening exponent.

Similar to the procedures adopted by the previous work of Leu (2005), we derive the analytical solutions as follows.

In the cylindrical coordinate system, the incompressibility condition requires that

$$\frac{\partial v}{\partial r} + \frac{v}{r} = 0 \tag{22}$$

where v is the radial velocity at a point (r,θ). Accordingly, the radial velocity can be expressed as

$$v = \frac{B}{r} \tag{23}$$

where B is a constant.

Accordingly, we can express the strain rates as

$$\dot{\varepsilon}_r = \frac{\partial v}{\partial r} = -\frac{B}{r^2} \tag{24}$$

$$\dot{\varepsilon}_\theta = \frac{v}{r} = \frac{B}{r^2} \tag{25}$$

$$\dot{\varepsilon}_z = 0 \tag{26}$$

and from Eqs. (24)∼(26) we obtain the equivalent strain rate

$$\dot{\bar{\varepsilon}} = \sqrt{\frac{2}{3}(\dot{\varepsilon}_r^2 + \dot{\varepsilon}_\theta^2 + \dot{\varepsilon}_z^2)} = \frac{2}{\sqrt{3}}\frac{B}{r^2} \tag{27}$$

Accordingly, the equivalent strain is obtained as

$$\bar{\varepsilon} = \int \dot{\bar{\varepsilon}} dt = \frac{1}{\sqrt{3}} \ln \frac{r^2}{r_0^2} \tag{28}$$

where r_0 is the initial radius to the location concerned.

The components of the stress deviator, s_r, s_θ, s_z, can be obtained by considering the flow rule and satisfying the yield condition. Thus, we obtain

$$s_r = -\frac{1}{\sqrt{3}}[\sigma_\infty - (\sigma_\infty - \sigma_0)\exp(-h\bar{\varepsilon})] \tag{29}$$

$$s_\theta = \frac{1}{\sqrt{3}}[\sigma_\infty - (\sigma_\infty - \sigma_0)\exp(-h\bar{\varepsilon})] \tag{30}$$

$$s_z = 0 \tag{31}$$

Thus, the stresses are given as

$$\sigma_r = s + s_r \tag{32}$$

$$\sigma_\theta = s + s_\theta \tag{33}$$

$$\sigma_z = s + s_z \tag{34}$$

where s is the mean normal stress.

Substituting Eqs. (32)∼(34) into the following equilibrium equation

$$\frac{\partial \sigma_r}{\partial r} + \frac{\sigma_r - \sigma_\theta}{r} = -\rho\omega^2 r \tag{35}$$

Therefore, we obtain

$$\frac{\partial \sigma_r}{\partial r} = -\frac{\sigma_r - \sigma_\theta}{r} - \rho\omega^2 r = \frac{2}{r}\left[\frac{\sigma_\infty}{\sqrt{3}} - \frac{\sigma_\infty - \sigma_0}{\sqrt{3}}\exp(-h\bar{\varepsilon})\right] - \rho\omega^2 r \tag{36}$$

Note that $h = \sqrt{3}$ is used in the derivations. Thus, with the boundary conditions $\sigma_r(r=a) = P_i$ and $\sigma_r(r=b) = P_o$, the limit value of the angular velocity factor $\rho\omega^2$ at the current radii a, b is given by

$$\rho\omega^2 = \frac{2}{b^2 - a^2}(P_i - P_o) + \frac{2}{b^2 - a^2}\left\{\frac{\sigma_0}{\sqrt{3}}\ln\frac{b^2}{a^2} - \frac{(\sigma_\infty - \sigma_0)}{\sqrt{3}}\left(\frac{a_0^2}{a^2} - \frac{b_0^2}{b^2}\right)\right\} \tag{37}$$

If the angular velocity factor $\rho\omega^2$ is normalized by σ_0/b_0^2, then we have the dimensionless angular velocity factor $\rho\omega^2 b_0^2/\sigma_0$ in the form as

$$\frac{\rho\omega^2 b_0^2}{\sigma_0} = \frac{2b_0^2}{b^2 - a^2}\left(\frac{P_i - P_o}{\sigma_0}\right) + \frac{2b_0^2}{b^2 - a^2}\left\{\frac{1}{\sqrt{3}}\ln\frac{b^2}{a^2} - \frac{(\sigma_\infty/\sigma_0 - 1)}{\sqrt{3}}\left(\frac{a_0^2}{a^2} - \frac{b_0^2}{b^2}\right)\right\} \tag{38}$$

Note that, the sign convention for P_i and P_o in Eqs. (37) and (38) is positive for tension and negative for compression.

Appendix B:

To consider instability and then the existence of the maximum value of the limit angular velocity during the whole widening process, we apply the necessary condition for the maximum of $\rho\omega^2 b_0^2/\sigma_0$, namely the following mathematical expression with the current interior radius a

$$\frac{\partial(\rho\omega^2 b_0^2/\sigma_0)}{\partial a} = 0 \tag{39}$$

Considering Eqs. (38) and (39), we get the condition of instability in the form

$$\frac{b_0^2 - a_0^2}{(\sigma_\infty/\sigma_0 - 1)} = \frac{a_0^2}{a^2}(a^2 + b_0^2 - a_0^2) - \frac{a^2 b_0^2}{(a^2 + b_0^2 - a_0^2)} \tag{40}$$

For convenience, we set

$$X = \frac{a^2 + b_0^2 - a_0^2}{a^2} = \frac{a^2 + b^2 - a^2}{a^2} = \frac{b^2}{a^2} > 1 \tag{41}$$

and

$$\begin{aligned} A &= \frac{b_0^2 - a_0^2}{(\sigma_\infty/\sigma_0 - 1)} \\ &= a_0^2 \frac{(b_0/a_0)^2 - 1}{(\sigma_\infty/\sigma_0 - 1)} \\ &= a_0^2 \overline{A} \end{aligned} \tag{42}$$

Then Eq. (40) can be rewritten as

$$X^2 - \overline{A}X - (b_0/a_0)^2 = 0 \tag{43}$$

Therefore, we have the explicit solution

$$X = \frac{\overline{A} + \sqrt{\overline{A}^2 + 4(b_0/a_0)^2}}{2} \tag{44}$$

When X has been obtained for given a_0/b_0 and σ_∞/σ_0 , the onset of instability can be identified from Eq. (41) as

$$\frac{a}{a_0} = \sqrt{\frac{(b_0/a_0)^2 - 1}{X - 1}} \tag{45}$$

Finally, we come to consider the condition of stability, namely the existence of hardening phenomena before the weakening behavior. Mathematically, it is to consider the case expressed in the form

$$\frac{\partial(\rho\omega^2 b_0^2/\sigma_0)}{\partial a} > 0 \tag{46}$$

Certainly, the condition expressed by Eq. (46) is equivalent to see if there is the solution $a/a_0 > 1$ to Eqs. (45). Therefore, we can get the stability condition, corresponding to the strain-hardening described by the Voce hardening law with $h = \sqrt{3}$, by Eqs. (42), (44) and (45) as

$$\sigma_\infty/\sigma_0 > 2 \tag{47}$$

Therefore, there exists strengthening phenomenon if rotating cylinders are made of hardening materials with $\sigma_\infty/\sigma_0 > 2$. Accordingly, the hardening behavior is to be observed in the range in the following expression

$$1 < \frac{a}{a_0} < \sqrt{\frac{(b_0/a_0)^2 - 1}{X - 1}} \tag{48}$$